Indonesian Journal of Electrical Engineering and Informatics (IJEEI)
Vol. 13, No. 2, June 2025, pp. 336~346
ISSN: 2089-3272, DOI: 10.52549/ijeei.v13i2.6114

Efficient Strategies for a Medium Voltage Loop Powered by an Infinite Source

Ethmane Isselem Arbih Mahmoud[1], Ahmed Abbou[2], Abdel Kader Mahmoud[3], Né Dah Eida[4]
[1,2,3] Research Team in Electrical Energy and Control, Mohammed V, University, Mohammadia School of Engineers, Morocco
[1,4] Unité de Recherche en Electromécanique et environnement'UREM-E', Institut Supérieur d'Enseignement Technologique (ISET), Rosso
[3] Unité de Recherche Appliquée aux Energies Renouvelables, Eau et Environnement (URA3E), FST, UN, Mauritania

Article Info

Article history:

Received Dec 8, 2024
Revised Apr 6, 2025
Accepted Apr 24, 2025

Keywords:

Infinite source
Transformers
Compensator
Circuit Breaker
MATLAB, PSS/E and ETAP

ABSTRACT

This paper analyzes and examines the potential of an infinite generation system to support the domestic load growth of the 33 kV loop network from 2025 to the year 2040. The study assesses the current state of the network, focusing on voltage levels, line loadings, and transformer capacities to ensure that all components operate within the system's allowable loading limits. It is assumed that the loop is powered by an infinite source. A numerical model, utilizing the Gauss-Seidel method, is developed and run using the PSS/E simulator and ETAP. The voltage profile is expected to remain within the range of 0.95 to 1.05 pu. An analysis of the simulation results demonstrates the potential for increasing active power transfer and controlling reactive power in the system by the year 2040.Furthermore, solutions are proposed to address identified critical issues in order to meet the projected demand. These include doubling the capacity of existing transformers and implementing protection against short-circuit currents. The proposed system is expected to provide industrial consumers with reduced load imbalances and improved control over voltage fluctuations caused by rapid changes in reactive power demand.

Corresponding Author:

Ethmane Isselem Arbih Mahmoud,
Department of electric Power Engineering,
Mohammed V University, Mohammadia School of Engineers,
Avenue : Ibn Sina B.P:765, Rabat -Morocco.
Email: ethmaneisselemarbih1966@gmail.com

1. INTRODUCTION

This study looks at whether an infinite source generation system can reliably supply electricity to homes through a 33 kV network, including during faults like short circuits [7,9]. The main goal is to keep the voltage levels between 0.95 and 1.05 per unit (pu). To do this, the power grid was modeled and tested using software tools like PSS/E, ETAP, and MATLAB to check whether it meets the voltage standards set by the grid operator. Other researchers have used different methods to address similar voltage and power flow problems. Some have used optimization techniques like Optimal Power Flow (OPF), while others have used artificial intelligence tools such as Genetic Algorithms or Particle Swarm Optimization. These methods can improve system performance but often require more complex calculations.

In contrast, this study uses simpler, well-established techniques like the Gauss-Seidel method for load flow analysis, which is easier to implement in medium-sized systems. The study also introduces a reactive power compensation system to help control voltage and power flow more efficiently under changing conditions [10–15]. Similar devices like SVCs and STATCOMs have been used in other studies to improve voltage stability, especially in high-voltage networks.

Here's how the study was carried out:

A diagram of the 33 kV network and system data for 2022 were presented [16–18].
The network's admittance matrix was calculated, and load flow analysis was performed.
Electricity demand from 2025 to 2040 was forecasted and analyzed.
A numerical model using the Gauss-Seidel method was built in MATLAB and PSS/E to simulate the system's behavior.
The results were used to find and solve system problems and improve power flow and voltage profiles. And lastly, the study emphasizes that upgrading transformer capacity and performing short-circuit simulations are key to building a stable and reliable electrical network [19,21].

2. RESEARCH METHOD

Figure 1 presents the single-line diagram of the 33 kV loop network. The corresponding line data, injected powers at the buses, and load information are detailed in tables 1 and 2, respectively. The network comprises four transmission lines, four transformer substations each powered by an infinite source and four loads connected to buses 1 through 4, as illustrated in the diagram. Active and reactive power values are represented in megawatts (MW) and megavolt-amperes reactive (MVAR), respectively. The voltage at each bus (i) is expressed in per unit (pu). Each load bus is characterized by a specified active power (P) and reactive power (Q), the voltage magnitude (V) at each bus is computed through power flow analysis. In this configuration, bus 3 is selected as the slack bus, providing a reference for system voltage and angle. Additionally, each bus (i) is interconnected with (k) other buses, forming a closed-loop structure as depicted in figure 1.

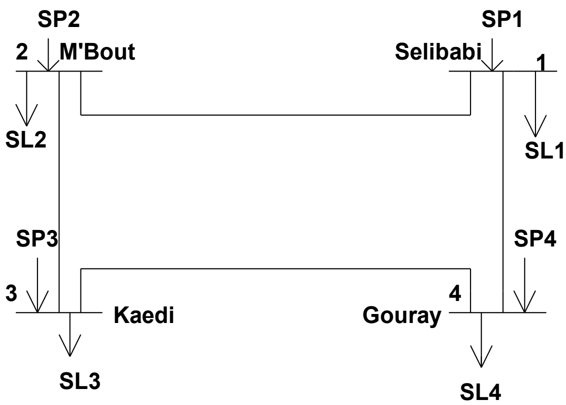

Figure 1. Single line diagram of the 33 KV loop system
Legend: SP - Substation power, SL - Power Load, 1 ;2 ;3; 4 Bus numbers

2.1. lines parameters

To express all the values in per unit (pu) as shown in table 1, two independent base quantities must be selected arbitrarily at a specific location within the electrical system commonly the base voltage U_B and base power S_B. These base values are then used to calculate the base impedance, which is derived using Ohm's law. The base impedance can be determined using the following formula

2.2. Calcululation of bases values

Base impedance in power systems is used when you're doing per-unit (pu) analysis. It acts as a reference value to normalize electrical quantities like voltage, current, and impedance. It helps simplify complex calculations. It allows you to compare components across different voltage levels and power ratings more easily. It keeps values in a similar range (usually around 1.0), which helps reduce errors. it's calculated by equation (1):

$$Z_B = \frac{U_B^2}{S_B} = \frac{(33^2)*1000}{800} = 1361\Omega \tag{1}$$

$with\ U_B = 33KV\ bus\ voltage\ and\ S_B = 800KVA\ is\ apparent\ power\ of\ transformer$ at 2022 year (table 2)
Once you have the base impedance, you can convert actual impedances to per-unit values and analyze the system more uniformly as shown in table 1.

Table 1. Line parameters

Bus (i – k)	Resistance (Ω)	Rpu=R/Z_B	Reactance (Ω)	Xpu =X/Z_B	Voltage (kV)	Length (km)
1-2	2,147	0,0015	2,9380	0,00215	33	113
2-3	2,0805	0,00152	2,847	0,00207	33	109,5
3-4	3,8247	0,00281	5,2338	0,00384	33	201,3
4-1	0,84816	0,00061	1,16064	0,000852	33	44,64

Table 2 provides data for the year 2022, including initial voltages, voltage angles, injected powers, and power demands. This information is essential for evaluating the performance and efficiency of the power distribution system. Analyzing these parameters supports efforts to ensure the network's reliability and operational stability.

Table 2. initial given data of the network

Bus no.	Bus voltage		Injected power		Load	
	Voltage magnitude (pu)	Angle (deg)	P (kW)	Q (kVAr)	P (kW)	Q (kVAr)
1	1.05	0	634,5	310,2	564	423
2	1	0	333	162,8	296	222
3	1	0	720	352	640	480
4	1	0	288	140,8	256	192

Table 3 presents the projected system demand from 2025 to 2040, estimated using extrapolation techniques. This forecast is crucial for strategic planning and efficient resource allocation. It enables the anticipation of future demand and supports proactive system upgrades.

Table 3. Projected demand of the system between 2022 and 2040 years

Country	2025 - 2030		2030- 2035		2035-2040	
	P_D (Mw)	Q_D (Mvar)	P_D (Mw)	Q_D (Mvar)	P_D (Mw)	Q_D (Mvar)
Sélibabi	10.33	7.524	11.537	8.653	13.268	9.951
M'Bout	4.751	4.345	5.464	4.997	6.284	5.746
Kaédi	11.385	8.538	13.09	9.819	15.056	11.292
Gouray	4.109	3.42	4.726	3.93	5.435	4.523
Total Powers	30,575	23,827	34,817	27,399	40,043	31,512

Table 4 presents the simulation results for the admittance matrix involving buses 1, 2, 3, and 4. This data highlights the electrical interactions and performance of these buses within the network. Analyzing these results is essential for understanding the system's dynamic behavior and ensuring stability.

Table 4. Admittance matrix of system

	1	2	3	4
1	0,7807 - j1,0695	-0,2206 + j0,3016	0	-0,5601 + j0,7679
2	-0,2206+ j0,3016	0,4472 - j0,6127	-0,2206+ j0,3016	0
3	0	-0,2267 +j 0,3111	0,3507 - j0,4807	-0,1241+ j0,1696
4	-0,5601 + j0,7679	0	-0,1241+ j0,1696	0,6842 - j0,9375

2.3. Calculation of bases values

Load flow studies are essential for effective power system planning and operation. The main objective is to calculate the voltage magnitudes and angles at each bus under specified generation and load conditions. To solve the load flow problem, we employed the iterative Gauss-Seidel method, using MATLAB and PSSE due to the manageable size of the system.

2.3.1. Gauss Seidel resolution

Using Kirchhoff's Current Law (KCL) from figure 1, we obtain the following equation:

$$\mathrm{I_i} = \mathrm{Y_{i1}V_1} + \mathrm{Y_{i2}V_2} + \cdots + Y_{ii}V_i + \cdots + \mathrm{Y_{in}V_n} = \sum_{\mathrm{k}=1}^{\mathrm{n}} \mathrm{Y_{ik}V_k} \tag{2}$$

The conjugate complex power at bus(i) is given by

$$\mathrm{P_i} - \mathrm{jQ_i} = \mathrm{V_i^* I_i} \tag{3}$$

Substituting equation (1) into equation (3), we obtain:

$$\mathrm{P_{i,inj}} - \mathrm{j}Q_{i,inj} = \mathrm{V_i^*} \sum_{\mathrm{k}=1}^{\mathrm{n}} V_{ik}V_k = \mathrm{V_i^*}[Y_{i1}V_1 + Y_{i2}V_2 + \cdots + Y_{ii}V_i + \cdots + Y_{in}V_n] \tag{4}$$

Then, the voltage at bus(i) is defined by equation (5)

$$\mathrm{V_i} = \frac{1}{\mathrm{Y_{ii}}}\left[\frac{\mathrm{P_{i,inj}} - \mathrm{jQ_{i,inj}}}{V_i^*} - \mathrm{Y_{i1}V_1} - \mathrm{Y_{i2}V_2} - \cdots - \mathrm{Y_{in}V_n}\right] \tag{5}$$

Calculation of current flowing between bus(i) and bus (k)

$$\mathrm{I_{ik}} = -\mathrm{Y_{ik}}(\mathrm{V_i} - \mathrm{V_k}), \quad \mathrm{i} \neq \mathrm{k} \tag{6}$$

Hence

$$\mathrm{V_i} = |\mathrm{V_i}|\angle\delta_\mathrm{i}, \ \mathrm{V_k} = |\mathrm{V_k}|\angle\delta_\mathrm{k}, \ \mathrm{Y_{ii}} = |\mathrm{Y_{ii}}|\angle\theta_\mathrm{ii}, \ \mathrm{Y_{ik}} = |\mathrm{Y_{ik}}|\angle\theta_\mathrm{ik} \tag{7}$$

$$\mathrm{P_i} - \mathrm{jQ_i} = \mathrm{V_i^* I_i} = \mathrm{V_i^*} \sum_{\mathrm{k}=1}^{\mathrm{n}} \mathrm{Y_{ik}V_k} = \sum_{\mathrm{k}=1}^{\mathrm{n}} |\mathrm{Y_{ik}V_iV_k}| \left(\cos(\theta_\mathrm{ik} + \delta_\mathrm{k} - \delta_\mathrm{i}) - \mathrm{j}\sin(\theta_\mathrm{ik} + \delta_\mathrm{k} - \delta_\mathrm{i})\right) \tag{8}$$

The injected powers at bus(i) are defined by equations (9) and (10)

$$\mathrm{P_i} = \sum_{\mathrm{k}=1}^{\mathrm{n}} |\mathrm{Y_{ik}V_iV_k}| \cos(\theta_\mathrm{ik} + \delta_\mathrm{k} - \delta_\mathrm{i}) \tag{9}$$

$$\mathrm{Q_i} = -\sum_{\mathrm{k}=1}^{\mathrm{n}} |\mathrm{Y_{ik}V_iV_k}| \sin(\theta_\mathrm{ik} + \delta_\mathrm{k} - \delta_\mathrm{i}) \tag{10}$$

Since the voltage at the buses must be maintained within certain specified statutory limits, the voltage bound constraint limit at bus (i) is defined by equation (11)

$$V_{i(\min)} \leq V_i \leq V_{i(\max)} \tag{11}$$

Where Vi (min) and Vi (max) are minimum and maximum voltage values at bus i.
The reactive power supply constraint at bus (i) is specified by equation (12)

$$Q_{gi(\min)} \leq Q_{gi} \leq Q_{gi(\max)} \tag{12}$$

With Qgi(min) et Qgi(max) are minimum and maximum reactive powers values generated at bus(i)

3. RESULTS AND DISCUSSION

3.1. Numerical model of resolution

Table 5 presents the simulation results from the PSS/E simulator for the year 2040, prior to the insertion of the reactive power compensator. The table displays the voltage magnitude profile and corresponding voltage angles across the system. The results show that voltage magnitudes fall below the acceptable stability range (0.95 to 1.05 pu) throughout the network, with the exception of the slack bus.

Table 5. Simulation results at 2040 year with using PSS/E

Name of Bus	N°	Type	Vpu	ϕ °
Selibabi	1	PQ	0.9	-1.55
M'Bout	2	PQ	0.93	-0.89
Kaedi	3	Slack	1	0
Gouray	4	PQ	0.91	-1.37

3.2. Model of reactive power compensation

Table 5 shows the simulation results from the PSS/E simulator without the implementation of reactive power compensation. The voltage magnitude profile and voltage angles are observed to fall outside the acceptable stability margin. To address this issue, we propose the following mathematical model for reactive power compensation:

$$Q_C = 3 * \omega * U^2 * C \quad Avec\ \omega = 2\pi f \tag{13}$$

Where, Qc- is a reactive power in MVAr, U - is a bus bar voltage, C - is a capacitance in µF, ω - is a pulse, F is a network frequence. Given that C= 20 µF, U=33KV, F=50Hz, we calculate the reactive power required to maintain the system within voltage constraints (0.95 and 1.05pu) substituting these values into equation (11) then applying equation (14).

$$Q_C = 3 * 314 * 33^2\, 10^6 * 20 * 10^{-6} = 20.51\ MVAR\ with\ \omega = 314\ rad/s \tag{14}$$

The injected reactive power at Selibabi bus bar (1) is Qc = 20.51 MVAR. This represents a bank of capacitors shunt or use Static Var Compensators (SVC) and STATCOM from the FACTS family for reactive power compensation connected at bus (1) .

3.3 Resolution of the problematic

Table 6 presents the simulation results for the voltage profile and angles following the insertion of the reactive power compensation system. The results show that the voltage values are now within the stability constraints (0.95 to 1.05 pu). The table below illustrates these improved conditions.

Table 6. Simulation results after injected reactive power at bus 1

Bus N°	Type	Vpu	ϕ °
Selibabi 1	PQ	1	-5.15
M'Bout 2	PQ	0.985	-2.69
Kaedi 3	Slack	1	0
Gouray 4	PQ	0.99	-4.33

Figure 2 illustrates the voltage profile before and after the reactive power compensation. It shows an increase in voltage magnitude at bus 1, from 0.90 (outside the [0.95, 1.05 pu] range) to 1 pu, at bus 2 from 0.93 to 0.98 pu, and at bus 4 from 0.93 to 0.99 pu. Notably, slack bus 3 maintained its voltage at 1 pu and its angle at 0°.

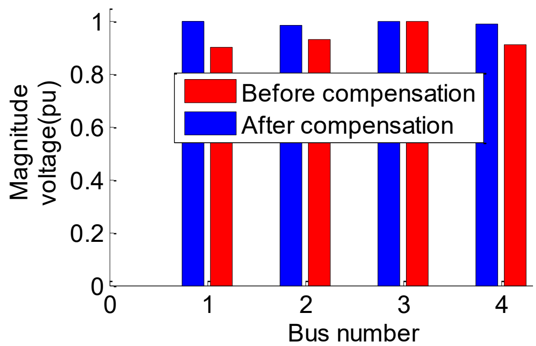

Figure 2. Curve of voltage magnitude in pu

Figure 3 shows the voltage angles before and after reactive power compensation. The results indicate an improvement in the voltage angle at Bus 1, from -1.55° to -5.15°, at bus 2, from -0.89° to -2.69°, and at bus 4, from -1.37° to -4.33°.

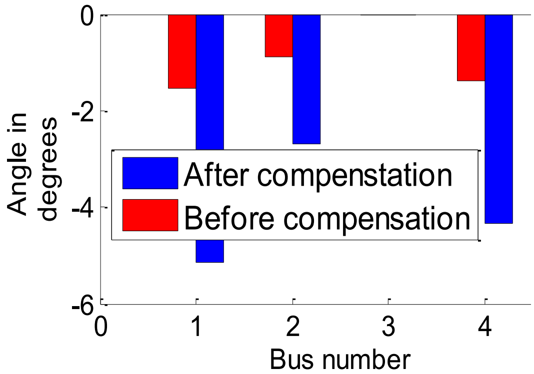

Figure 3. Curve of voltage angle in degrees

Table 7 presents the simulation results for total active and reactive power before and after the insertion of the reactive power compensation system at the Selibabi bus (Bus 1). A reduction in total power losses is observed, demonstrating the effectiveness of the compensation system. This improvement highlights the system's contribution to overall network efficiency.

Table 7. The total active and reactive power losses

Method	Active Power losses (MW)	Reactive Power losses (MVAR)
Before compensation	1.8	2.5
After compensation	1.5	2

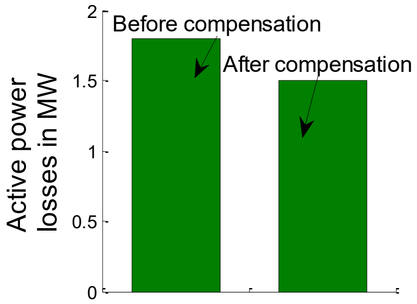

Figure 4. Total active power losses

Figure 4 shows a reduction in total active power loss from 1.8 MW to 1.5 MW, indicating an improvement in active power transmission through the lines. This reduction highlights the effectiveness of the reactive power compensation system. The results demonstrate how the system enhances voltage levels at the buses and reduces active power losses..

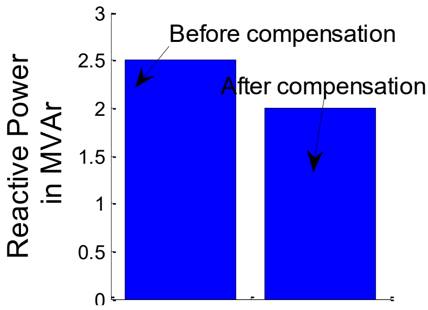

Figure 5. Total reactive power losses

Figure 5 shows a reduction in total reactive power loss from 2.5 MVAR to 2 MVAR, indicating a decrease in reactive power loss through the transmission lines. These results highlight the effectiveness of the reactive power compensation system. The system contributes to enhancing voltage levels at the buses while reducing reactive power losses in the power system.

3.4. Transformer Model

To address the projected load growth of the 33 kV loop network by the year 2040, we propose increasing the capacity of the transformers connected to various system buses [22]. This enhancement can be achieved by connecting one or more additional transformers in parallel with the existing units[23-25]. Parallel transformer operation is typically employed when the load demand exceeds the capacity of a single transformer, enabling an increase in available power without altering the system voltage. In such configurations, the power demand is shared between the parallel units. Connecting transformers in parallel also offers operational and economic benefits. It reduces the need for maintaining a large inventory of spare parts, as identical units can serve as mutual backups. Moreover, parallel operation improves system reliability, facilitates more efficient switching operations, and ensures continuity of power supply in the event of a transformer outage [26–28].

The cost associated with maintaining spare parts is reduced when two transformers are connected in parallel. The advantages of parallel transformer operation include meeting load demand, improved reliability, more efficient switching operations, and an uninterrupted power supply during the outage of one unit[29]. For transformers to operate effectively in parallel, several technical conditions must be satisfied [30–33]:

Identical primary and secondary voltage ratings: Both transformers must have the same voltage ratio and turns ratio.

Consistent transformation ratio (k): The ratio of primary to secondary voltage must be the same for both units.

Matching short-circuit impedance: The short-circuit voltage should be equal, or at least not exceed 10%.

Compatible phase displacement: The phase angle shift between primary and secondary windings must be identical; i.e., the vector groups must be the same or compatible.

By ensuring these conditions are met, parallel transformer operation becomes a practical and efficient solution to support future increases in load demand within the 33 kV network.

3.4.1. Model parallel operation of transformers

To share the total load between two transformers connected in parallel, the following information is required:

The power rating of transformer T1 (MVA1) and its percentage impedance (%Z1).

The power rating of transformer T2 (MVA2) and its percentage impedance (%Z2).

The total demand power (MVA).

With these parameters, the load can be appropriately distributed between the two transformers.

Load sharing by T1

$$T1 = \frac{\frac{MVA1}{\%Z1}}{\frac{MVA1}{\%Z1}+\frac{MVA2}{\%Z2}} * MVA \tag{15}$$

Equation of current crossing T1

$$I_1 = \frac{\frac{MVA1}{\%Z1}}{\frac{MVA1}{\%Z1}+\frac{MVA2}{\%Z2}} * I_L \tag{16}$$

Load sharing by T2

$$T2 = \frac{\frac{MVA2}{\%Z2}}{\frac{MVA1}{\%Z1}+\frac{MVA2}{\%Z2}} * MVA \tag{17}$$

Equation of current crossing T2

$$I_2 = \frac{\frac{MVA1}{\%Z1}}{\frac{MVA1}{\%Z1}+\frac{MVA2}{\%Z2}} * I_L \tag{18}$$

Where the percentage impedance is expressed by equation(18)

$$\%Z = \frac{Z_{Tr}}{U_{Tr}^2} * S_n * 100 \tag{19}$$

impedance of transformer $Z_{Tr} = \frac{U_{CC}}{100} * \frac{U_{20}^2}{S_n}$; $R_{Tr} = \frac{P_{Cu}}{3I_n^2}$; $X_{Tr} = \sqrt{Z_{Tr}^2 - R_{Tr}^2}$ (20)

The apparent power losses in the transformer can be calculated using the expression for each transformer(21)

$$\Delta S_{T1} = S_{T1\,input} - S_{T1\,output} \tag{21}$$

Where $S_{T1\,input}$ is the input power of transformer one and $S_{T1\,output}$ the output power of the same tranformer.

To assess the load-sharing performance of transformers connected in parallel at bus 3 (Kaédi) in the year 2040, we analyze both simulated and analytical cases. The power and current values distributed between the two transformers are determined using equations (15) to (18), with supporting data presented in tables 3, 8, and 9. In this configuration, one transformer (T1) is already installed, with a power rating of 10 MVA. As the projected total load demand exceeds this capacity, a second transformer (T2) is proposed to operate in parallel. The required power rating for T2 can be calculated as the difference between the total load demand and the existing transformer's capacity.

The total load demand (MVA) minus the power rating of the existing transformer (MVA1) gives the load that needs to be handled by the second transformer (MVA2).

Mathematically: MVA2 = Total Load Demand (MVA) − MVA1 (22)

Where: MVA1 is the power rating of the existing transformer (10 MVA). MVA2 is the power rating required for the second transformer. To validate the transformer load-sharing strategy, the study considers two approaches:

Simulation Case: The PSS/E software is used to simulate the total load demand of the network at bus 3 in the year 2040. This provides a realistic model based on the system's operational conditions and projected demand profile.

Analytical Case: Using equations (15) to (22), the load and current shared between T1 and T2 are calculated analytically. These calculations account for transformer ratings and impedance characteristics, and the results are documented in tables 8 and 9.
This dual-approach enables a direct comparison between simulated load demand and theoretical load-sharing predictions, offering valuable insights into the reliability and accuracy of the proposed transformer configuration.

Based on tables 8 and 9, we can determine and allocate the shared load between the two transformers, with T1 rated at 10 MVA and T2 rated at 30.04 MVA for the year 2040. Operating the transformers in parallel proves to be more economical than replacing them, as this approach allows for scalable load handling. This strategy effectively accommodates load increases while maintaining system stability[34-36].

Table 8. Calculation results of load shared at Kaedi bus (3)

Bus	Total load (T) (MVA)	Load of existing (T1) (MVA1)	Load shared by (T2) (MVA2)	Impedances of T1 and T2 %Z1	%Z2
Kaedi (3)	40.04	10	30,04	9	12,5
Year	2040	< 2030	> 2030	-	-

The simulation results are presented in table 9, where the apparent losses for each transformer are calculated. The upstream and downstream powers of each transformer are determined using equation (21). Additionally, the Kirchhoff's Current Law (KCL) in equation (2) is verified.

Table 9. Simulation results of apparent power losses at Kaedi bus (3)

Bus	Simulations results MVA				Simulations results of currents in (A		
	T1	T2	ΔS_{T1}	ΔS_{T2}	T1	T2	Total
Kaedi (3)	11.99	25.9	0,57	1,41	219.8	474.7	694,2

To protect transformers from short circuits, circuit breakers with adequate interrupting capacity must be selected. This can be achieved by simulating short circuit scenarios using ETAP, both upstream and downstream of the transformers. The simulation results will help identify the appropriate circuit breakers, ensuring their interrupting capacity is greater than or equal to the short circuit currents, as outlined in equations (23) and (24).

$$I_{CC} = \frac{U_0}{\sqrt{3}\, Z_T} \tag{23}$$

Where $Z_T = \sqrt{\sum R^2 + \sum X^2}$ is the total impedance upstream of the transformer, U0 is the voltage in secondary winding of transformer, I_{CC} is a short circuit current in KA.

$$I_{CC\,max} \leq B.C \tag{24}$$

Where B.C is a breaking capacity of electrical device in KA

Table 10 shows the results of both calculations (using equation 23) and a simulation (using ETAP software) for a short circuit situation. A short circuit current is the very large current that flows when electricity takes an unexpected shortcut, like when wires touch directly or connect to the ground with little resistance. This causes a sudden spike in current. When we compare these short circuit currents to the normal operating currents in table 8, we can see they are much higher which is normal in a fault condition. Also, the calculated short circuit current is higher than the simulated one. This difference can happen because manual calculations often assume ideal conditions, while simulation software includes more real-world details like resistance in wires and equipment behavior.

Table 10. Simulation results for the short circuit case using ETAP

Bus N°	Calculated values		Simulated results		
	Icc(KA)	B.C	Icc(KA)	V(%)	B.C
1	1.9	≥ 1.9	1.283	0	≥ 1.283
2	3.5	≥ 3.5	2.477	0	≥ 2.477

4. CONCLUSION

In this paper, we examined the state of a 33 kV loop over two distinct periods. The analysis focused on system stability, voltage levels, and power flow. Each period represents a different operational scenario with unique challenges and solutions. In the first period, we analyzed the network parameters for the year 2022. During this time, the system remained stable. All voltage and power levels were within the required standards. In the second period, we projected the demand from 2025 to 2040. The forecast showed that the system would exceed stability limits. To address this, we proposed injecting reactive power using a FACTS device of STATCOM at the Selibabi bus (Bus 1).

This intervention helps maintain voltage levels within the acceptable range of 0.95 to 1.05 per unit. It also reduces power mismatches under increased demand. As a result, the system operates more reliably. In another scenario, we considered transformer overloading[36] due to increased load. Operating transformers in parallel proved to be more economical. This method avoids full replacements by adding transformers as needed. The parallel operation supports load growth while maintaining system stability. When demand decreases, one transformer can be turned off. This improves efficiency during periods of low load.

Lastly, we extended the study to include a short-circuit analysis. This step ensures the protection of transformers. We selected appropriate circuit breakers to safeguard the system.

ACKNOWLEDGMENTS

The authors would like to thank the Rosso Higher Institute of Technological Education, Electromechanical Engineering Department, in Mauritania, Research Team in Electrical Energy and Control, Department of electric Power Engineering, Mohammadia School of Engineers, Mohammed V, University, Laboratory of Research Applied to Renewable Energies, Nouakchott, University, Mauritania. We also extend our gratitude to the reviewers for their valuable remarks, which have significantly improved the quality of this paper.

REFERENCES

[1] *L. Lilien, "Cours transport et distribution de l'énergie électrique," PhD. Dissertation, Institut de l'électricité Mont fore, Université de liège, 2013.*

[2] F. G. Merconchini, L. V. Seisdedos, J. C. Oliva, J. R. N. Alvarez and D. C.-Cervantes, "Study of electric power quality indicators by simulating a hybrid generation system," *International Journal Power Electronics & Drive System,* vol. 14, no. 2, pp. 1044-1054, 2023.

[3] M. Hamoud, A. M. A. Soliman and S. K. Elsayed, "Optimal power flow using Archimedes optimizer algorithm," *International Journal Power Electronics & Drive System*, vol. 13, no. 3, pp. 1390-1400, 2022.

[4] A. Rezaei1, A. Balal and Y. P. Jafarabadil, “Using machine learning prediction to design an optimized renewable energy system for a remote area in Italy,” International Journal of Applied Power Engineering, vol. 12, no. 3, pp. 331-340, 2023.

[5] L. K. Sahoo1 and M. Ray, “Energy Management Analysis of Residential Building Using ANN Techniques,” *Indonesian Journal of Electrical Engineering and Informatics*, vol. 11, no. 3, pp. 854-869, 2023.

[6] K. Adeleye, D. O. Akinyele and A. O. Amole, “Voltage Rise Problem in Distribution Networks with Distributed Generation: A Review of Technologies, Impact and Mitigation Approaches,” *Indonesian Journal of Electrical Engineering and Informatics,* vol. 9, no. 3, pp. 575-600, 2021,

[7] M.T. Sarker, M. J. Alam, G. Ramasamy and M. N. Uddinl, “Energy demand forecasting of remote areas using linear regression and inverse matrix analysis,” *International Journal Electrical & Computer Engineering*, vol.14, no.1, pp. 129-139, 2024.

[8] I. A. Ethmane Mahmoud, M. Maaroufi and A.Kader Mahmoud “Optimization for Electric Power Load Forecast,” *International Journal Electrical & Computer Engineering*, vol.8, no.5, pp. 3453-3462, 2018.

[9] E. Almeshaiei and H. Soultan, “A methodology for Electric Power Load Forecasting,” *Alexendria Engineering Journa*l, pp.137-144.

[10] M. Myintzu1 and K. Zin Oo, “Optimal capacitor allocation for minimizing cost of energy loss in active distribution network with different load levels,” *International Journal of Applied Power Engineering*, vol. 12, no. 1, pp. 71-82, 2023.

[11] M. O. Oyeleye and O. Adeyemo, “Reliability Evaluation of 33/11kv Olunde Injection Substation for Improved Performance,” *Indonesian Journal of Electrical Engineering and Informatics*, vol. 10, no. 1, pp. 165-176, 2022.

[12] M. Mahmoud and A. Fazal. “Reliability improvement of power systems using shunt reactive compensation and distributed generation,” *International Journal of Applied Power Engineering*, vol. 12, no. 3, pp. 277-292, 2023.

[13] P. R. Kumari, K. Rajasri and T. D. S.Reddy, “Power factor improvement using silicon-based switching devices for changing load parameters,” *Internationa Journal of Applied Power Engineering*, vol. 12, no. 4, pp. 367-372, 2023.

[14] E. Albanna, A. Ahmed and A. A, Al-Karakch. “Active and reactive energy storage STATCOM distribution system power management,” *International Journal Power Electronic & Drive Systems*, vol.15, no. 1, pp. 261-270, 2024.

[15] I. A Ethmane Mahmoud, A. Yahfdhou, A.K. Mahmoud, and M. Maaroufi,“Statcom integration in a power grid to enhance voltage stability,”*Indonesian Journal of Electrical Engineering and Informatics,* vol. 7, no. 4, pp. 620-627, 2019.

[16] T.S. Tran, T.-Huyen Dang and A.-Tung Tran, “Optimal Control of Switched Capacitor Banks in Vietnam Distribution Network Using Integer Genetic Algorithm,” Indonesian Journal of Electrical Engineering and Informatics, vol. 11, no. 2, pp. 553-561, 2023.

[17] A. D. Hermawan, I. Y. Negara and C. S. A. Nandar, “Effect of the placement capacitor bank on electrical power quality in the ILST fan drive system,” *International Journal Power Electronics & Drive System*, vol.15, no. 3, pp. 1435-1445, 2024,

[18] M.A. Al-Tak , M. F. Ain and O. Sh. Al-Yozbaky, “Impact of grading capacitor on transient recovery voltage due to shunt reactor de-energization for different values of current chopping,” *International Journal Power Electronics & Drive System*, vol.15, no. 2, pp. 1300-1307, 2024.

[19] N. Agouzoul, A. Oukennou, F. Elmariami, J. Boukherouaa and R. Gadal, “Power efficiency improvement in reactive power dispatch under load uncertainty,” *International Journal Electrical & Computer Engineering,* vol. 14, no. 4, pp. 3616-3627, 2024.

[20] Y.-W. Liu et al., "Improvement of power quality by using advanced reactive power compensation,"*2018 IEEE Trans on Ind Appl, vol. 54, no. 1*, pp. 18–24, Jan. 2018.

[21] Z. Cabrane, M.Maaroufi and M. Ouassaid, “Batteries and supercapacitor for photovoltaic energy storage: a fuzzy logic management,” IET-Renewable Power Generation, vol.11, no 8, pp. 1157-1165, 2017.

[22] N. S. I. Razali, T. S. Gunawan and S. H. Yuso, “Voltage Instability and Voltage Regulating Distribution Transformer Assessment Under Renewable Energy Penetration,” *International Journal Electrical & Computer Engineering*, vol. 11, no. 3, pp. 673-684, 2023.

[23] I. Onyebuchi and N.1, Dahunsi, “Enhancement of Power Supply with Paralleling of Transformers Using Same Parameters Approach,” *International Research Journal of Engineering and Technology*, vol.7, no 11, pp. 397-404, 2020.

[24] B. Bugra and N.Pamuk. “Theoretical and practical analysis of parallel operating conditions of two transformers with different relative short circuit voltages,” *Sigma Journal Engineering and Natural Sciences*, vol. 42, no. 4, pp. 1-18, 2024.

[25] D. Trebolle1 and B. Valecillos, “Optimal Operation of Paralleled Power Transformers,” *Renewable Energy and Power Quality Journal*, vol. 6, no.1, pp.1-6, 2008.

[26] Z. W. Aung, “Analysis of Three Phase Transformer Parallel Operation and Circulating Current,” *International Journal of Trend in Scientific Research and Developement*, vol. 3, no 5, pp. 1147-1150, 2019.

[27] K. M.I. Dadenkov, M. I. Kuznetsov and D. A. Dadenkov, “Parallel operation of three-phase power transformers with different short-circuit voltages,” *Russian. Electrical. Engineering.* vol. 88, no 6, pp. 388–393, 2017,

[28] R. A.V., Kuznetsov and D. A. Dadenkov, “Transformation of reactive power in a three-circuit transformer with capacitive compensation,” *Russian. Electrical Engineering,* vol. 84, no.11, pp. 595–598, 2013.

[29] M. State Electricity Distribution Company Limited, “*Technical Specification of 5 MVA and 10 MVA Power Transformer*,’’ 2019, pp.1-94.

[30] B. Gasbaoui, “ *Optimisation de l’énergie réactive dans un réseau d'énergie électrique*,’’ Université Bechar - Algérie, 2008, pp.57-66.

[31] Catalogues transformateurs, "*Transport et distribution de l'énergie électrique*,'' Nexans.www.nexans.ma. 2015, pp.1-32.
[32] *Schneider Electric, Power- and-Distribution- Transformers*, Australian catalogue, 2014, pp.1-32.
[33] D. Nilly, "*Le diagnostic d'état des transformateurs de puissance*,'' CNAM, CENTRE D'ENSEIGNEMENT D'AIX-EN-PROVENCE, 2017, pp.1-136.
[34] N. Rashid, "*Short-time Overloading of Power Transformers,*'' Royal Institute of Technology, Department of Electrical Engineering ABB Corporate Research, Stockholm, Sweden 2011, pp. 1-107.
[35] D. AL-hamad and K. Buruncuk, "*Implimantation methods to eliminate overload power system problem*,'' Near East University, Faculty of Engineering, Department of Electrical & Electronics Engineering, Nicosia, Turkish ,Republic of Northern Cyprus, pp.1-5,
[36] A. Bin-Halabi, A. Nouh and M. Abouelela, "A Simple and Effective Strategy to Prevent Power Transformer Overloading,'' *American Scientific Research Journal for Engineering, Technology, and Sciences*, vol.48, no. 1, pp.201-214, 2018.

BIOGRAPHY OF AUTHORS

Ethmane Isselem Arbih Mahmoud Dr. Ethmane Isselem Arbih was born in Tidjikja, Mauritania, in 1966.He received Master of Sciences degree in electrical systems and networks from Ukraina-Vinnitsa state university in 1994. and his PhD degree in electrical engineering from the University of Mohammad V (UM5R) of Rabat in Morocco, in 2019. Currently is an assistant professor at the High Technological Educational Institute of Rosso country, Mauritania. His current research interests include, Power Systems and Energy Efficiency and automatic control and renewable energies and artificial intelligence (NN, ML, DL...) for power system application. Author of seven (7) manuscripts, two (3) conferences and two books. He can be contacted at email: ethmaneisselemarbih1966@gmail.com.

Ahmed ABBOU He received the B.E. degree from ENSET in Rabat, the M.E. degree from Mohammed V University in Rabat and the Ph.D. degree from Mohammed V University in Rabat, in 2000, 2005 and 2009, respectively, all in electrical engineering. Since 2009, he has been working at Mohammadia School of engineers, Mohammed V University in Rabat, Department of electric Power Engineering, where he is a full Professor of Power Electronics and Electric drives. He published numerous papers in scientific international journals and conferences proceedings. His current research interests include induction machine control systems, self-excited induction generator, power electronics, sensorless drives for AC machines, Electric Vehicles charge, drone control and renewable energy conversion. He can be contacted at email: abbou@emi.ac.ma

Abdel Kader Mahmoud was born in Aleg, Mauritania in 1960. He received his Master degree of sciences in power stations in 1988 and his PhD degree in electrical engineering from the Technical University of Tashkent in Uzbekistan, in 1991. Then he received his second doctorate degree in renewable energy from the University of Cheikh anta Diop (UCAD), Dakar, Senegal, in 2008. Currently he is in charge of the Applied Research Laboratory of Renewable Energy (LRAER). He is the author and co-author of more than 30 scientific papers. Their current project is 'Comparison between the different numerical models and determination of parameters characteristics physical materials. He can be contacted at email: nakader@yahoo.fr